A Theoretical Study of the Low-Lying States of the Anionic and Protonated Ionic Forms of Urocanic Acid

Christopher S. Page*

Departamento de Quìmica Fìsica, Universitat de València, Dr. Moliner 50, Burjassot, E-46100 València, Spain

Massimo Olivucci

Dipartimento di Chimica, Università degli Studi di Siena,via Aldo Moro, I-53100 Siena, Italy

Manuela Merchán

Departamento de Quìmica Fìsica, Universitat de València, Dr. Moliner 50, Burjassot, E-46100 València, Spain

A multistate second-order perturbation theory (MS–CASPT2) study of the lowest lying states in the electronic spectra of urocanic acid in vacuo is presented. The anionic trans and cis isomers, as well as the biologically important trans protonated ionic structure, are considered. The vertical and 0–0 excitation spectra were computed for each system at the MS–CASPT2/ANO-L level, describing the lowest lying $\pi\pi^*$ and $n\pi^*$ singlet and triplet states. In all three systems, a weakly absorbing $\pi\pi^*$ singlet state was observed at ~4.0 eV in the vertical excitation spectrum, suggesting both a novel assignment and an alternative explanation for the previously described wavelength dependent photochemistry of this molecule. The trans anion vertical spectrum otherwise comprises three intense $\pi\pi^*$ transitions, at 4.14, 4.59, and 5.00 eV, whereas that of the cis anion shows two, at 4.52 and 5.01 eV. Conversely, the vertical spectrum of the protonated trans system is dominated by a single, intensely absorbing $\pi\pi^*$ state, computed at 4.76 eV. The wave functions of the $\pi\pi^*$ states all show a multiconfigurational character, which is most pronounced in the protonated ionic structure. The lowest vertical singlet states are of $n\pi^*$ character (trans anion, 4.13 eV; cis anion, 3.81 eV; trans protonated, 3.19 eV), although the lowest triplet states are due to $\pi\pi^*$ transitions (trans anion, 3.40 eV; cis anion, 3.39 eV; trans protonated, 2.56 eV). In each of the anionic systems, the origin of the most intense singlet $\pi\pi^*$ transition in the vertical spectrum (trans anion, 4.03 eV; cis anion, 3.81 eV) lies below the corresponding lowest singlet $n\pi^*$ vertical excitation energy, further suggesting that the latter state may not be directly and efficiently populated. Good agreements with available experimental data are noted throughout.

1. Introduction

Urocanic acid (4-imidazoleacrylic acid; Figure 1) occurs naturally as the trans isomer, a product of the metabolic deamination of histidine by the enzyme histidase. In the mammalian liver, it acts as a substrate for the enzyme urocanase. Urocanase is, however, absent in the epidermis, and there is an accumulation of urocanic acid as a consequence: although excreted with sweat, it has been found to account for 0.7% of the dry-weight of the human *stratum corneum*.[1,2]

In recent years, urocanic acid has been the subject of a great deal of attention, due to its importance in photodermatology. It is a major UV chromaphore, exhibiting strong absorption in the UV-B region (300–280 nm, 4.13–4.43 eV). UV-B irradiation is known to bring about lesions in DNA at neighboring pyrimidines, a process that may lead ultimately to skin cancer.[3] Indeed, *trans*-urocanic acid has an absorption spectrum so remarkably similar to the epidermal photocarcinogenic action spectrum[4] that for a number of years it was included in artificial sunlotions. It was withdrawn from such use in the early 1990s,

following the discovery that the *cis*-isomer, a prevaling UV-B photoproduct, has a selective immunosuppressive role, being an analog of the immunoregulator histamine.[5] With immunosuppression being linked to tumor growth, this has thus led to the ironic conclusion that, far from being a "natural sunblock", urocanic acid may actually be implicated in photocarcinogenesis, via a UV-B induced photoisomerization.[6] Other effects of this immune suppression include a down-regulation of contact and delayed-type hypersensitivity,[7] and an alteration in the morphology and function of the epidermal Langerhans cells.[8]

Structurally, urocanic acid has three protonation sites—the carboxylic moeity and the tertiary and secondary nitrogens—that have been assigned pK_a's of 3.5, 5.8, and 13.0, respectively.[9] Accordingly, urocanic acid is neutral at pH < 3.5, but exists as a protonated ionic structure in the range pH 3.5–5.8, and as the carboxylate anion in the range pH 5.8–13. It follows that, while it forms the anion in aqueous solution, the tertiary nitrogen is protonated in the human skin, which has a pH gradient of ~4–6.[10]

Besides its intrinsic biological importance, the photochemistry of *trans*-urocanic acid has proved to be interesting, and somewhat controversial. While its absorption spectrum exhibits

---

Ionic Forms of Urocanic Acid

J. Phys. Chem. A, Vol. 104, No. 38, 2000 **8797**
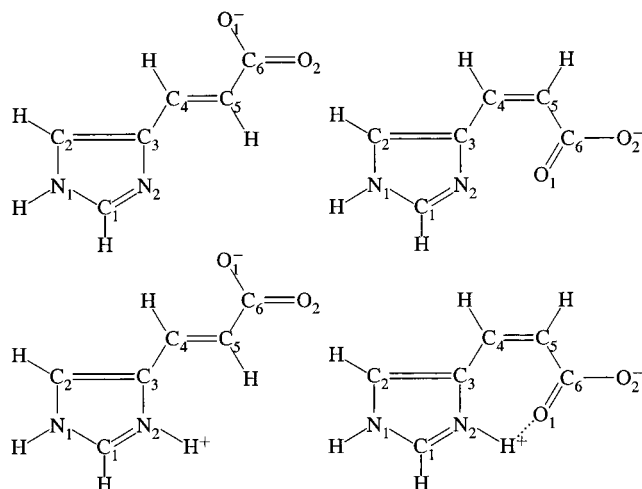
Figure 1. Schematic representations of the (top) carboxylate anions and the (bottom) N_2 protonated ions of *trans-* and *cis*-urocanic acid. The cis protonated form is not considered in this paper (see text for discussion).

a broad peak with a maximum at ~4.4 eV,[11,12] the quantum efficiency of the isomerization process peaks at ~4.0 eV ($\psi_{E \to Z}^{4.0eV} = 0.52$; $\psi_{E \to Z}^{4.0eV} = 0.49$, cf. $\psi_{E \to Z}^{4.7eV} = 0.05$; $\psi_{E \to Z}^{4.7eV} = 0.08$).[13] The spectrum also shows a shoulder at ~5.5 eV.[11] *cis*-Urocanic acid has an absorption spectrum that is virtually superposable with the trans isomer, albeit with an extinction coefficient that is reduced by up to 30%.[12] The photostationary state reached is typically enriched in the cis form (85% in vitro, 55% in vivo).[1]

Hanson, Li and Simon discuss two possible explanations for the wavelength dependence in isomerization efficiency.[12,14] The first of these is that the broad, structureless UV spectrum may arise from a superposition of differing spectra due to a number of ground-state rotamers, which in turn each have different reactivities. This view was taken by Shukla and Mishra in an earlier paper, based on the results of semiempirical CNDO/S−CI calculations in support of their spectroscopic study.[11] The alternative hypothesis, for which Hanson and Simon have recently provided substantial evidence, is that the absorption spectrum is a consequence of multiple electronic states with overlapping absorption transitions that are not easily distinguished, and that it is excitation to one or other of these states that gives rise to the differing activities.[15] This latter view is concurrent with the behavior observed in the urocanic acid analog, cinnamic acid:[13,16] in this case, the absorption spectrum is dominated by a $\pi\pi^*$ transition from the phenyl ring, with a weak $n\pi^*$ transition contributing to the red tail (<4.1 eV) of the profile.

The absorption spectrum for *trans*-urocanic acid shows a maximum (oscillatory strength of 10^4) at 4.45 eV at pH 5.6, which is red shifted to 4.30 eV at pH 7.2.[12] Excitation in the range 4.4−4.7 eV leads to peak fluorescence.[11,14] The fluorescence spectrum has a $\pi\pi^*$ maximum at 3.5 eV, irrespective of pH. Li et al. attribute these observations to a $\pi\pi^*$ transition, localized on the imidazole ring.[14] That there is a common excited state at pH 5.6 and 7.2, indicated by the pH invariance of emission, is thought to be due to a reduction of the electron density on the tertiary nitrogen brought about by the transition, lowering the pK_a and leading to a rapid deprotonation (τ < 200 fs). This singlet state is believed to be short-lived (τ < 7 ps), subsequently undergoing an intersystem crossing to a relatively long-lived (τ > 10 ns) triplet, which has been shown by both triplet sensitization and photoacoustic calorimetry to have an

energy of 2.4−2.6 eV.[12,17] The rate constant of this process was measured at 1.4×10^{11} s^{-1}.

Hanson et al., note, however, that following excitation at 4.0 eV, the maximum emission is at 3.3 eV at pH 7.2 and at 3.2 eV at pH 5.6.[12] In the latter case, the maximum varies with excitation wavelength in the range 3.9−4.1 eV. These findings are thought to be due to a singlet $n\pi^*$ excitation. The lifetime of the emitting singlet is short (<40 ps) at both pHs as a consequence of rapid, nonradiative decay. In this case, there is no indication of any decay to a triplet state, intersystem crossing being slow in comparison to isomerization. Morrison et al., have further shown that low and high energy triplet quenchers have no effect on isomerization.[17] Hanson et al., conclude that under physiological conditions, isomerization occurs via the singlet manifold.

The sum of $\psi_{Z \to E}$ and $\psi_{E \to Z}$ is unity,[12] the quantum efficiency of photodegradation small (0.001).[17] This implies that isomerization is the primary event following photoexcitation at 4.0 eV. The rate-limiting steps for each pathway (trans → cis and cis → trans) have almost identical kinetic parameters, suggesting further that there is a common transient state.[18]

The quantum efficiencies of trans → cis isomerization show a slight pH dependence, increasing as the pH is raised from 3.0 to 7.4, then declining. However, Hanson and Simon suggest that their "data indicate that [*trans*-urocanic acid] exhibits identical wavelength-dependent photochemistry regardless of pH"[12] and that "the insensitivity of pH is consistent with the observation that the general photoreactivity observed upon excitation at 264 and 310 nm is not influenced by the protonation state of [the] tertiary nitrogen in the imidazole ring".[15]

One major source of confusion, especially in theoretical studies, concerns the existence of an intramolecular hydrogen bond in the cis conformer.[19,20] In aqueous solution, this is unlikely to form, due to competition from the solvent molecules: the molecule will clearly not prefer a single intramolecular N−H···O=C hydrogen bond when it can form both N−H···OH$_2$ and multiple HO−H···O=C intermolecular interactions without suffering any contortions. Furthermore, from the authors' own recent calculations of the spectra of the two neutral isomers in vacuo,[21] it was shown that formation of the hydrogen bond leads to a marked red shift in the spectrum of the cis isomer relative to that of the trans, an observation that is quite inconsistent with the experimental finding that the two spectra of the solvated species are "virtually superposable". This in turn would imply that the most stable forms of both anionic isomers are protonated at the same site on the imidazole ring, contrary to the structures considered, e.g., by Lahti et al.[20,22,23]

Presented in this paper are the results of ab initio calculations of the low-lying singlet and triplet states of the trans and cis isomers of the urocanic acid anion, and of the trans isomer of the urocanic acid protonated ion. The study includes geometry optimizations of the ground and lowest lying excited states. The states have been characterized using multiconfiguration second-order perturbation theory.[24,25] In addition, the indirect interaction of the resulting states has been taken into account within the framework of the multistate CASPT2 (MS−CASPT2) protocol. These data serve both to complement the earlier study of the neutral species, and to provide a firm foundation for a theoretical elucidation of the isomerization pathway.

2. Methods and Computational Details

The trans and cis isomers of anionic urocanic acid, and the trans isomer of the protonated ionic form, as depicted in Figure 1, were considered.

TABLE 1: CASSCF Wave Functions Used to Compute the Valence Transitions of Anionic trans/cis and Protonated Ionic trans Urocanic Acid

wave function	$N_e{}^a$	state	no. of conf^b	$N_{states}{}^c$
vertical spectra (ANO-L basis set)				
CASSCF (F: 10−0. I: 19−0. A: 1−10.)^d	14	$1^1A'$	18100	1
CASSCF (F: 10−0. I: 20−0. A: 0−10.)^d	12	$5^1A' (\pi\pi^*)$	13860	7
		$1-3^3A' (\pi\pi^*)$	20790	3
CASSCF (F: 10−0. I: 19−0. A: 1−10.)^d	14	$1^1A'' (n\pi^*)$	13860	1
		$1^3A'' (n\pi^*)$	23100	1
geometry optimizations (6-31+G(d) basis set)				
CASSCF (I: 30−1. A: 0−8.)^e	10	$1-2^1A' (\pi\pi^*)$	1176	1 or 2
		$1^3A' (\pi\pi^*)$	1512	1
CASSCF (I: 29−2. A: 1−7.)^e	10	$1^1A'' (n\pi^*)$	1176	2
		$1^3A'' (\pi\pi^*)$	1512	1

^{a} Number of active electrons. ^{b} Number of configurations in the CASSCF wave function. ^{c} States included in the average CASSCF wave function. ^{d} Within parentheses the number of frozen (F), inactive (I), and active (A) orbitals of symmetry, of the point group. ^{e} Within parentheses the number of inactive (I) and active (A) orbitals of the point group.

Consideration of the N_2 protonated cis isomers was deliberately avoided in this work. While energetically favored in the gas phase, their stability derives from an intramolecular hydrogen bond that, in the view of the authors, would not form in polar protic solvents. This point effectively precludes a realistic theoretical analysis of the cis isomer of the urocanic acid protonated ion without the inclusion of both a dielectric continuum and explicit solvent molecules in the model; such a treatment is beyond the current scope. Where appropriate, comparison shall be made between the trans anion and protonated ion, and reasonable extrapolations proposed.

2.1. Wave Functions. A full list of the CASSCF wave functions used in the course of this work is given in Table 1.

The closed-shell HF descriptions of both the $C_6H_5N_2O_2{}^-$ and $C_6H_6N_2O_2$ systems have (30−6) occupied orbitals of symmetry $(a'-a'')$. The π orbitals belong to the a'' irreducible representation of the point group C_s.

In general, for the singlet and triplet states of A' symmetry, the π-valence active space (0−10) has been employed (10π active orbitals with 12π active electrons), for what will henceforth be referred to as the π-CASSCF wave function. For the $\pi\pi^*$ states, the lone-pairs of the heteroatoms behave as inactive orbitals: it is found that the occupation numbers are close to 2.0 when they are treated as active.

For the 1,3A''(nπ^*) states the active space also included the carboxylate lone-pair (i.e. (1−10) with 14 active electrons), identified by inspection of the HF orbitals.

2.2. Geometry Optimizations. Geometry optimizations for the ground-state and lowest-lying excited states were carried out at the CASSCF level using the 6-31+G(d) basis set. To assess the effects of dynamical correlation on geometry, analogous optimizations of the ground states were also performed at the MP2/6-31+G(d) level.

For geometry optimizations of states of A' symmetry, an active space was selected to include the energetically highest five (of six) π-valence molecular orbitals, determined from calculations at the SCF level, and the lowest three unoccupied orbitals of a'' symmetry.

The active spaces for the respective A'' state optimizations were similarly specified, with the exception that, for each structure, the lowest active π-valence electron pair was substituted for the carboxylate lone pair.

Full geometry optimizations to default tolerances were performed assuming planar structures with C_s symmetry (27 degrees of freedom for the anion, 29 for the ionic structure). The validity of the symmetry constraint was verified for the trans anion ground state by optimization from a severely distorted nonplanar starting geometry.

2.3. Vertical Spectra. The CASSCF optimized geometries for the ground states were employed in the calculation of the vertical excitation energies of the two anionic isomers and of the trans protonated ion.

Calculations were carried out at the CASSCF level using the generally contracted basis sets of the Atomic Natural Orbital (ANO-L) type, obtained from the C,N,O(14s9p4d)/H(8s) primitive sets.[26] The contraction scheme C,N,O[4s3p1d]/H[2s] was used in the present study,[27] comprising a total of 190 basis functions (192 for the protonated ionic structure).[28] To take into account the remaining correlation effects, the CASSCF wave functions were employed as reference functions in a single-state second-order perturbation CASPT2 treatment.[24,25] The coupling of the CASSCF wave functions via dynamic correlation was evaluated using the extended multistate CASPT2 approach, the MS−CASPT2 method.[29] An effective Hamiltonian matrix is constructed whereby the diagonal elements correspond to the CASPT2 energies and the off-diagonal elements introduce the coupling to second order in the dynamic correlation energy. In this way, all states of a given symmetry can be treated simultaneously with the correlation effects on the reference functions included. The molecular orbitals for the excited states were obtained from state average CASSCF calculations,[30] where the averaging included all states of interest of a given symmetry. The number of states included in the state average CASSCF calculations, the number of configurations in the CASSCF wave function, details of the active spaces used, and the types of states computed are given in Table 1.

The relative energy of each excited state is referred to a ground-state energy computed with the same active space. The carbon, nitrogen, and oxygen 1s electrons were kept frozen in the form determined by the ground-state HF wave function. All electrons except the core electrons were correlated at the CASPT2 level.

The CASSCF state interaction (CASSI) method[31,32] was used to compute the transition dipole moments μ_{ij} from the corresponding perturbation-modified CAS (PMCAS) reference functions,[29] that is, the model states, linear combinations of all CAS states involved in the MS−CASPT2 calculation. Oscillator strengths were computed employing these μ_{ij} values and the vertical excitation energies employed at the MS−CASPT2 level.[27,33,34]

2.4. Band Origins and Flourescence/Phosphorescence Energies. Band origins (0−0 energies) and flourescence/phosphorescence energies were computed for the lowest lying $n\pi^*$ and $\pi\pi^*$ transitions for anionic trans and cis and protonated ionic trans urocanic acid by calculating the ground state and vertical excitation energies for the $n\pi^*$ and $\pi\pi^*$ optimized

Ionic Forms of Urocanic Acid

J. Phys. Chem. A, Vol. 104, No. 38, 2000 **8799**

TABLE 2: Equilibrium Geometries for the Ground and Excited States of *trans*-Urocanic Acid Optimized at the MP2 and CASSCF Levels (6-31+G(*d*) Basis Set, Constrained C_s Symmetry)

bond/angle[a]	$1^1A'$		$2^1A'$	$1^3A'$	$1^1A''$	$1^3A''$
	MP2	CASSCF				
N_2-C_1	1.325	1.298	1.297	1.283	1.291	1.279
C_1-N_1	1.370	1.358	1.402	1.374	1.362	1.352
N_1-C_2	1.380	1.380	1.310	1.389	1.392	1.397
C_2-C_3	1.390	1.372	1.439	1.430	1.391	1.390
C_3-N_2	1.391	1.387	1.371	1.418	1.409	1.405
C_3-C_4	1.456	1.465	1.393	1.377	1.423	1.423
C_4-C_5	1.349	1.346	1.387	1.491	1.403	1.416
C_5-C_6	1.527	1.527	1.533	1.508	1.381	1.399
C_6-O_1	1.271	1.243	1.234	1.242	1.232	1.228
C_6-O_2	1.273	1.240	1.229	1.238	1.404	1.385
C_1-H	1.083	1.071	1.069	1.072	1.072	1.074
C_2-H	1.082	1.069	1.070	1.067	1.067	1.069
C_4-H	1.091	1.077	1.075	1.074	1.076	1.077
C_5-H	1.090	1.077	1.074	1.073	1.070	1.075
N_1-H	1.013	0.992	0.996	0.991	0.991	0.991
$N_2-C_1-N_1$	111.69	112.34	110.85	113.88	113.33	113.62
$C_1-N_1-C_2$	107.10	106.40	108.51	106.58	106.06	106.10
$N_1-C_2-C_3$	106.08	106.26	105.53	105.62	106.42	105.91
$C_2-C_3-N_2$	109.20	108.85	108.40	107.38	107.86	107.77
$C_3-N_2-C_1$	105.94	106.15	106.71	106.54	106.33	106.61
$C_2-C_3-C_4$	126.32	126.59	124.90	128.27	129.43	128.64
$C_3-C_4-C_5$	125.99	126.27	124.87	125.97	123.18	125.80
$C_4-C_5-C_6$	122.28	122.89	121.40	120.99	123.18	122.01
$C_5-C_6-O_1$	116.87	116.96	115.03	115.75	132.37	131.78
$C_5-C_6-O_2$	114.19	114.33	113.98	115.39	114.78	114.01
N_2-C_1-H	125.83	125.41	127.36	124.80	124.72	124.86
C_1-N_1-H	126.53	126.63	125.36	126.40	126.97	126.62
N_1-C_2-H	122.36	122.41	124.21	123.12	122.29	122.19
C_3-C_4-H	117.23	116.13	118.42	118.65	117.27	116.40
C_4-C_5-H	120.65	120.43	120.07	119.43	119.04	119.96

[a] Bond lengths in angstroms; angles in degrees.

TABLE 3: Equilibrium Geometries for the Ground and Excited states of *cis*-Urocanic Acid Optimized at the MP2 and CASSCF levels (6-31+G(*d*) Basis Set, Constrained C_s Symmetry)

bond/angle[a]	$1^1A'$		$2^1A'$	$1^3A'$	$1^1A''$	$1^3A''$
	MP2	CASSCF				
N_2-C_1	1.322	1.296	1.292	1.281	1.292	1.291
C_1-N_1	1.373	1.362	1.408	1.380	1.365	1.365
N_1-C_2	1.377	1.375	1.375	1.385	1.387	1.390
C_2-C_3	1.396	1.377	1.377	1.440	1.396	1.397
C_3-N_2	1.386	1.382	1.382	1.411	1.399	1.401
C_3-C_4	1.463	1.471	1.471	1.380	1.423	1.427
C_4-C_5	1.359	1.354	1.354	1.502	1.413	1.428
C_5-C_6	1.530	1.533	1.533	1.518	1.390	1.400
C_6-O_1	1.261	1.231	1.231	1.230	1.222	1.216
C_6-O_2	1.279	1.248	1.248	1.244	1.402	1.388
C_1-H	1.083	1.071	1.071	1.072	1.072	1.072
C_2-H	1.083	1.070	1.070	1.068	1.068	1.069
C_4-H	1.096	1.083	1.083	1.081	1.080	1.081
C_5-H	1.092	1.079	1.079	1.076	1.073	1.079
N_1-H	1.013	0.992	0.992	0.991	0.990	0.991
$N_2-C_1-N_1$	112.13	112.54	112.54	114.24	113.19	113.14
$C_1-N_1-C_2$	106.67	106.07	106.07	106.08	105.95	106.01
$N_1-C_2-C_3$	106.22	106.46	106.46	105.82	106.46	106.36
$C_2-C_3-N_2$	109.20	108.74	108.74	107.21	107.84	107.79
$C_3-N_2-C_1$	105.78	106.19	106.19	106.65	106.55	106.69
$C_2-C_3-C_4$	121.22	121.92	121.92	123.63	123.91	125.25
$C_3-C_4-C_5$	135.68	136.19	136.19	136.69	137.17	135.45
$C_4-C_5-C_6$	134.27	134.94	134.94	133.71	133.50	132.51
$C_5-C_6-O_1$	118.83	118.79	118.79	118.51	134.66	135.29
$C_5-C_6-O_2$	111.76	112.19	112.19	112.32	112.70	111.47
N_2-C_1-H	125.51	125.26	125.26	124.56	125.03	124.92
C_1-N_1-H	126.85	126.85	126.85	126.71	127.06	126.81
N_1-C_2-H	122.13	122.22	122.22	123.03	122.40	122.22
C_3-C_4-H	110.09	109.63	109.63	111.89	110.71	111.78
C_4-C_5-H	114.10	113.91	113.91	112.36	113.27	114.00

[a] Bond lengths in angstroms; angles in degrees.

geometries, in a manner entirely analogous to the vertical spectrum computation.

CASSCF/MS−CASPT2 and CASSI calculations were performed using the MOLCAS 4.1 quantum chemistry software.[35] Geometry optimizations employing the 6-31+G(*d*) basis set at the MP2 and CASSCF levels were carried out using the Gaussian 94 suite.[36] Default convergence criteria implemented in the respective programs were used throughout.

All calculations were carried out on the SGI Origin 2000 server of the University of Valencia.

3. Results and Discussion

3.1. Geometries. The atom numbering scheme used throughout this study of urocanic acid is defined in Figure 1.

The optimized geometric data for the ground and lowest lying $\pi\pi^*$ and $n\pi^*$ singlet and triplet electronic excited states of anionic trans and cis urocanic acid are given in Tables 2 and 3, respectively. Corresponding data for the ground and electronic excited states of the protonated trans urocanic acid ion are given in Table 4. All optimizations were constrained to C_s symmetry.

The difference in energies between the ground-state trans and cis anions calculated at the CASSCF/6-31+G(*d*) level is 12.26 kCal mol^{-1} in favor of the trans. This compares most favorably with an experimental estimate[12] of $\simeq$10 kcal mol^{-1}, and lends further weight to the authors' belief that previous studies implicating an intramolecular hydrogen bond in the cis geometry have been in error.

As with the previous work on the neutral species,[21] it was again found that the ground-state geometries obtained show a remarkable dependence on the correlation treatment employed,

with deviations in bond lengths as high as 0.03 Å between CASSCF and MP2. In this case, it is perhaps even more striking that MP2 consistently computes larger interatomic distances, within both the imidazole ring and within the carboxylate moiety, where a double bond has been formally assigned. Conversely, the C_3-C_4 bond is contracted by $\sim$0.01 Å, while *all* covalent bonds involving hydrogens are extended by at least the same order of magnitude. These effects may be attributed to overestimation of the extent of conjugation by the single reference correlated wave function,[37] and only the CASSCF geometries shall be considered further.

Comparison of the bond angles in the two anionic isomers suggests that the cis geometry is somewhat distorted by a N···O repulsion that, as with the deliberately precluded hydrogen bond, is purely an artifact of the model. Specifically, both the $C_3-C_4-C_5$ and $C_4-C_5-C_6$ angles are deformed by as much as 10°, with a reciprocal compression of angles C_3-C_4-H and C_4-C_5-H. There is also a more pronounced difference between the $C_5-C_6-O_1$ and $C_5-C_6-O_2$ in the cis anion than there is in the trans. In reality, solute−solvent interactions would act to stabilize the charge imbalance.

The protonated trans geometry is little different to that of the trans anion, save for the inevitable alterations in the bond lengths and angles implicating N_2, and a shortening of the C−O bond lengths due to charge stabilization.

An examination of the planar electronic excited-state geometries does not yield any surprising results. $^1A'$ and $^3A'$ and geometries show most significant changes with respect to the ground state occurring within the imidazole ring, whereas the $1^1A''$ state has a C_6-O_2 distance that is elongated by 0.15 Å in

TABLE 4: Equilibrium Geometries for the Ground and Excited states of the Protonated Ionic Structure of *trans*-Urocanic Acid Optimized at the CASSCF Level (6-31+G(d) Basis Set, Constrained C_s Symmetry)

bond/angle[a]	$1^1A'$	$2^1A'$	$1^3A'$	$1^1A''$	$1^3A''$
N_2-C_1	1.319	1.378	1.396	1.309	1.328
C_1-N_1	1.320	1.412	1.386	1.304	1.302
N_1-C_2	1.385	1.380	1.359	1.405	1.386
C_2-C_3	1.367	1.373	1.371	1.389	1.390
C_3-N_2	1.387	1.391	1.402	1.416	1.405
C_3-C_4	1.455	1.404	1.424	1.406	1.397
C_4-C_5	1.344	1.413	1.362	1.397	1.400
C_5-C_6	1.534	1.545	1.460	1.411	1.424
C_6-O_1	1.234	1.229	1.383	1.214	1.357
C_6-O_2	1.233	1.218	1.184	1.378	1.248
C_1-H	1.068	1.063	1.061	1.069	1.068
C_2-H	1.067	1.068	1.068	1.062	1.066
C_4-H	1.074	1.076	1.073	1.072	1.073
C_5-H	1.081	1.075	1.073	1.071	1.076
N_1-H	0.997	0.991	0.992	0.995	0.996
N_2-H	0.999	0.992	0.990	0.995	0.995
$N_2-C_1-N_1$	107.77	106.70	105.04	109.00	107.80
$C_1-N_1-C_2$	109.42	108.14	110.21	109.58	110.50
$N_1-C_2-C_3$	107.16	108.28	109.01	106.87	107.17
$C_2-C_3-N_2$	104.88	108.14	106.29	103.48	103.42
$C_3-N_2-C_1$	110.77	108.75	109.45	111.06	111.11
$C_2-C_3-C_4$	131.50	127.97	127.78	134.59	132.97
$C_3-C_4-C_5$	124.38	126.30	125.36	123.84	124.37
$C_4-C_5-C_6$	122.45	119.39	123.45	123.64	124.37
$C_5-C_6-O_1$	115.19	112.66	115.61	129.32	117.61
$C_5-C_6-O_2$	113.10	113.18	125.05	114.20	125.05
N_2-C_1-H	126.10	126.84	127.74	125.41	126.01
C_1-N_1-H	124.71	125.32	124.54	124.63	124.34
N_1-C_2-H	122.17	123.09	122.14	121.56	121.79
C_3-N_2-H	124.17	126.50	126.06	124.06	124.50
C_3-C_4-H	116.93	118.92	115.64	116.70	116.21
C_4-C_5-H	122.26	121.66	122.41	121.01	121.68

[a] Bond lengths in angstroms; angles in degrees.

both anionic isomers; similar effects may also be observed in the protonated analogs. The $1^3A''$ geometries are, for the most part, all but identical to the corresponding $1^1A''$, with bond lengths typically differing by less than 0.01 Å. Exceptions to this are slightly less pronounced C_6-O_2 elongations in the two anionic systems, and the fact that it is the C_6-O_1 that is extended in the protonated form.

From the point of view of isomerization, it is interesting to note that the $1^1A''$ geometries show both large contractions of the C_5-C_6 bond and elongations of $C_4=C_5$, suggesting significant changes in the bonding between these atoms that are not observed in the $^1A'$ states.

Intriguingly, however, there is an even greater lengthening (by as much as 0.15 Å) of the C_4-C_5 bond lengths in the anionic $1^3A'$ structures, which again indicates a marked weakening of the double bond. This effect is also observed, but not nearly so pronounced, in the protonated $1^3A'$ geometry.

3.2. Vertical Spectra of Urocanic Acid. Compiled in Tables 5 and 6 are the computed vertical excitation energies at the PMCAS−CI and MS−CASPT2 levels of theory, together with the oscillator strengths, and the contributions to the PMCAS-CI wave functions of the states, respectively, for the trans isomer of the urocanic acid anion. Corresponding data for the cis isomer of the urocanic acid anion may be found in Tables 7 and 8. Similarly, Tables 9 and 10 list the results for the protonated trans structure.

Figure 2 shows plots of the six highest occupied and four lowest unoccupied orbitals, together with their respective canonical orbital energies, computed at the self-consistent field (SCF) level. Corresponding electron density difference and

TABLE 5: PMCAS−CI and MS−CASPT2 Calculated Excitation Energies (eV) and Oscillator Strengths for Anionic *trans*-Urocanic Acid

state	excitation energy		oscillator strength
	PMCAS−CI	MS−CASPT2	
singlet states			
$1^1A''$ ($n\pi*$)	4.41	4.13	0.0003
$2^1A'$ ($\pi\pi*$)	6.80	4.14	0.1127
$3^1A'$ ($\pi\pi*$)	6.65	4.59	0.3038
$4^1A'$ ($\pi\pi*$)	6.32	5.00	0.2609
$5^1A'$ ($\pi\pi*$)	6.89	5.60	0.0034
6 ($\pi\pi*$)	6.47	6.11	0.0282
triplet states			
$1^3A'$ ($\pi\pi*$)	2.85	3.40	
$1^3A''$ ($n\pi*$)	4.33	4.02	
$2^3A'$ ($\pi\pi*$)	4.03	4.52	
$3^3A'$ ($\pi\pi*$)	5.04	5.41	

natural orbital plots for the vertical excitations relative to the respective ground states, computed at the PMCAS−CI level, are shown in Figures 3−6.

The vertical absorption spectrum of anionic trans urocanic acid, computed up to ∼6 eV, shows three strong $\pi\pi*$ electronic transitions, at 4.14 eV (oscillator strength 0.113), 4.59 eV (0.304), and 5.00 eV (0.261). The close spacing in the energy of these three states, taken together with their oscillator strengths, would suggest that the experimentally observed single broad peak, centered at 4.30 eV, is a superposition of these absorptions. Two additional, relatively weak electronic transitions, involving the $5^1A'$ and $6^1A'$ excited states, are to be found at 5.60 and 6.11 eV, respectively. These could be related to the "shoulder" that has been observed at 5.5 eV,[11] but that has otherwise attracted scant attention in the literature.

As with the neutral species, analysis of the A' PMCAS-CI wave functions for this structure reveals a multiconfigurational character, albeit one where doubly excited configurations make only a small contribution. Taking the 6a″ orbital as the HOMO (H) and the 7a″ as the LUMO (L), it can be seen that the wave functions of the lowest lying states are primarily composed of H → L, H − 1 → L, H → L + 1, H − 1 → L + 1 transitions.

Unlike previous studies which "permitted" the hydrogen bond, the calculated vertical excitation energies, and the corresponding wave functions, for the cis urocanic acid anion are very similar to those of the trans isomer, concurrent with the experimental finding that the two spectra are "virtually superposable". (A red shift of ca. 1.0 eV has been computed for the hydrogen bonded neutral species[21]). The four lowest lying $\pi\pi*$ states have vertical excitation energies of 3.85 eV (oscillator strength 0.044), 4.52 eV (0.481), 5.01 eV (0.124), and 5.36 eV (0.037). It is notable here that both the $2^1A'$ and $4^1A'$ have oscillator strengths that are roughly half those of the corresponding transitions in the trans isomer, whereas the intense $3^1A'$ and weak $5^1A'$ are somewhat enhanced. This is in contrast to the experimentally observed spectra, which show a lowering in absorption intensity of roughly 30%. The $6^1A'$ state is almost unchanged, at 6.23 eV (oscillator strength 0.021).

Assignment of electronic transitions within the cis anion in terms of SCF. orbitals shows an almost exact correspondence with the trans isomer: again, the wave functions for each of the states considered mainly comprise H → L, H − 1 → L, H → L + 1, and H − 1 → L + 1. The multiconfigurational character is more notable, but still doubly excited configurations make only a small contribution (cf. Tables 6 and 8).

The $1^1A''$ $n\pi*$ state is found at 4.13 and 3.81 eV, with trivial oscillator srengths, for the trans and cis urocanic acid anions, respectively. The lower energy computed for the cis isomer may

Ionic Forms of Urocanic Acid

J. Phys. Chem. A, Vol. 104, No. 38, 2000 **8801**

TABLE 6: PMCAS−CI Wave Functions for Anionic *trans*-Urocanic Acid: Principal Configurations,[a] Weights, and Number (weights) of Singly (S), Doubly (D), and Triply (T) Excited Configurations[b] with Coefficients Larger than 0.05

state	principal configurations	%	no. of configurations (weights)		
			S	D	T
$1^1A'$	...4a''29a'30a'5a''6a''	83.9	2 (5.2%)	9 (4.7%)	
singlet states					
$1^1A''$	29a' → 8a''	91.7	1 (91.7%)	1 (0.4%)	6 (3.8%)
$2^1A'$	5a' → 8a''	75.3	6 (87.3%)	6 (3.3%)	2 (0.7%)
$3^1A'$	6a' → 7a''	57.4	10 (85.2%)	4 (2.1%)	
	6a' → '8a''	13.3			
$4^1A'$	6a' → 7a''	69.7	9 (83.3%)	6 (3.9%)	3 (1.0%)
$5^1A'$	5a' → 7a''	79.4	3 (86.4%)	3 (1.3%)	8 (4.4%)
$6^1A'$	6a' → 9a''	42.6	9 (69.0%)	17 (19.9%)	1 (0.5%)
	4a' → 8a''	18.4			
triplet states					
$1^3A'$	6a' → 8a''	46.6	7 (90.2%)	1 (0.3%)	5 (2.9%)
	6a' → 9a''	23.7			
	4a' → 9a''	11.8			
$2^3A'$	6a' → 8a''	26.5	9 (86.5%)	4 (3.2%)	5 (1.7%)
	6a' → 9a''	23.0			
	4a' → 8a''	18.0			
$3^3A'$	4a' → 9a''	40.8	9 (84.0%)	8 (5.2%)	5 (3.0%)
	3a' → 8a''	14.2			
	4a' → 9a''	14.0			
$1^3A'$	29a' → 8a''	91.8	1 (91.8%)	1 (0.4%)	6 (3.9%)

[a] Those with weights > 10%. [b] With respect to the ground-state principal configuration.

TABLE 7: PMCAS−CI and MS−CASPT2 Calculated Excitation Energies (eV) and Oscillator Strengths for Anionic *cis*-Urocanic Acid

state	excitation energy		oscillator strength
	PMCAS−CI	MS−CASPT2	
singlet states			
$1^1A''$ ($n\pi^*$)	4.13	3.81	0.0003
$2^1A'$ ($\pi\pi^*$)	6.66	3.85	0.0437
$3^1A'$ ($\pi\pi^*$)	7.18	4.52	0.4813
$4^1A'$ ($\pi\pi^*$)	6.38	5.01	0.1244
$5^1A'$ ($\pi\pi^*$)	6.83	5.36	0.0369
$6^1A'$ ($\pi\pi^*$)	6.57	6.23	0.0213
triplet states			
$1^3A'$ ($\pi\pi^*$)	3.02	3.39	
$1^3A'$ ($n\pi^*$)	4.04	3.68	
$2^3A'$ ($\pi\pi^*$)	4.16	4.45	
$3^3A'$ ($\pi\pi^*$)	5.21	5.43	

to some extent be an artifact of the N···O repulsion inherent in the model, as noted above.

While these data compare most favorably with the experimental finding that peak isomerization efficiency is observed following excitation at 4.0 eV, supporting the view that photoexcitation of the carboxylate lone pair leads to isomerization, the near-degeneracies with the respective $2^1A'$ states of the two anions cannot be overlooked. Indeed, of the two possibilities, the $\pi\pi^*$ transition is the predominant in terms of absorption efficiency, albeit having a shorter lifetime. On the basis of this evidence, therefore, it seems more plausible that isomerization follows from excitation to the $2^1A'$ electronic excited state. The wavelength dependency of the photoisomerization may then be attributed to the "dark" $2^1A'$ state having a quite different relaxation path to the more strongly absorbing $4^1A'$.

TABLE 8: PMCAS−CI Wave Functions for Anionic *cis*-Urocanic Acid: Principal Configurations,[a] Weights and Number (weights) of Singly (S), Doubly (D), and Triply (T) Excited Configurations[b] with Coefficients Larger than 0.05

state	principal configurations	%	no. of configurations (weights)		
			S	D	T
$1^1A'$	...4a''29a'30a'5a''6a''				
singlet states					
$1^1A''$	30a' → 8a''	91.6	1 (91.6%)	1 (0.5%)	6 (3.8%)
$2^1A'$	5a'' → 8a''	84.2	5 (87.1%)	7 (3.9%)	1 (1.4%)
$3^1A'$	6a'' → 8a''	77.0	11 (84.6%)	6 (4.0%)	1 (0.5%)
$4^1A'$	6a'' → 7a''	78.2	6 (85.4%)	4 (2.3%)	3 (1.3%)
$5^1A'$	5a'' → 7a''	81.2	2 (86.4%)	2 (0.8%)	5 (3.5%)
$6^1A'$	6a'' → 9a''	29.2	11 (66.4%)	18 (22.4%)	2 (0.6%)
	4a'' → 8a''	27.9			
triplet states					
$1^3A'$	6a'' → 8a''	58.8	7 (89.9%)	3 (0.9%)	5 (3.2%)
	4a'' → 9a''	10.8			
$2^3A'$	6a'' → 9a''	27.6	8 (86.6%)	5 (3.1%)	3 (1.0%)
	4a'' → 8a''	18.0			
	6a'' → 8a''	16.4			
	3a'' → 8a''	10.2			
$3^3A'$	4a'' → 9a''	42.2	8 (84.5%)	6 (3.9%)	5 (2.8%)
	3a'' → 8a''	13.1			
$1^3A''$	30a' → 8a''	91.7	1 (91.7%)	1 (0.4%)	8 (4.2%)

[a] Those with weights >10%. [b] With respect to the ground-state principal configuration.

8802 *J. Phys. Chem. A, Vol. 104, No. 38, 2000*

Page et al.

TABLE 9: PMCAS−CI and MS−CASPT2 Calculated Excitation Energies (eV) and Oscillator Strengths for Protonated Ionic *trans*-Urocanic Acid

	excitation energy		
state	PMCAS-CI	MS-CASPT2	oscillator strength
singlet states			
$1^1A''$ $(n\pi^*)$	2.61	3.19	0.0000
$2^1A'$ $(\pi\pi^*)$	2.69	3.04	0.0155
$3^1A'$ $(\pi\pi^*)$	3.25	3.57	0.0023
$4^1A'$ $(\pi\pi^*)$	4.43	4.10	0.0707
$5^1A'$ $(\pi\pi^*)$	5.59	4.76	0.4666
$6^1A'$ $(\pi\pi^*)$	6.31	5.83	0.0141
triplet states			
$1^3A'$ $(\pi\pi^*)$	2.73	2.56	
$2^3A'$ $(\pi\pi^*)$	2.81	2.97	
$1^3A''$ $(n\pi^*)$	2.59	3.13	
$3^3A'$ $(\pi\pi^*)$	3.52	3.63	

The case of the protonated trans urocanic acid ionic structure (Tables 9 and 10, and Figures 2, 3 and 6) is interesting, in that the three lowest lying $\pi\pi^*$ states have significantly lower (~1.0 eV) excitation energies and oscillator strengths compared to their counterparts in the spectrum of the trans anion, having been computed at 3.04 eV (oscillator strength 0.016), 3.57 eV (0.002) and 4.10 eV (0.071). Instead, only one intense state is observed, at 4.76 eV (oscillator strength 0.467). A weak shoulder is again predicted, at 5.83 eV (oscillator strength 0.014).

This can be understood most easily by consideration of electron density differences: the transitions in the protonated form are very different in character to those of the anions, and invariably result in a migration of density from the carboxylate moeity to the imidazole ring, although it is unclear to what extent this would be moderated by the inclusion of a solvation treatment in the calculations. Similarly, whereas the natural orbital plots for the two anions mirror each other closely, it is almost impossible to assign analogs between the plots for the protonated structure and those for the trans anion.

It is, however, interesting to note that this is despite near-identical topographies of the canonical orbitals between the two trans species, albeit with quite different relative and absolute energies. Indeed, if one accepts that the topology of the 5a″

HF orbital of the protonated trans makes it "equivalent" with the 6a″ of the anion, it can be seen first that the most intense electronic transitions in both spectra ($5^1A'$ in the protonated structure; $3^1A'$ in the anion) share essentially the same principal configurations. By the same line of reasoning, the $3^1A'$ in the protonated system may be deemed to be the closest analog of the $2^1A'$ in the anion. The variation in the excitation energies of these states between the two structural forms (3.57 eV for the protonated ion; 4.14 eV for the anion) may then account for the pH dependence of isomerization efficiency.

Otherwise, the wave functions for the protonated species also display a number of important differences in character compared to the anions. Although again mainly comprising H → L, H − 1 → L, H → L + 1, and H − 1 → L + 1 configurations, the importance of doubly excited contributions is more remarkable, particularly in the $3^1A'$ (12%), $5^1A'$ (19%) and $6^1A'$ (69%) states. Moreover, the wave functions of the electronic excited states $4^1A'$ and above cannot be attributed to any single primary configuration.

The $1^1A''$ state is calculated at 3.19 eV for the protonated trans structure, red-shifted by almost 1.0 eV relative to the trans anion. This may again be due to the fact that the protonated species was treated in vacuo, and it is conceivable that the inclusion of solvation terms would significantly alter this. Nevertheless, it is worth reiterating that the experimentally derived quantum efficiency of 4.0 eV photoinduced isomerization *increases* with pH, and it is not possible to reconcile this with the computed $1^1A''$ excitation energies. On this basis it again seems reasonable to suggest that the $1^1A''$ state plays no part in the isomerization.

Computed $1^3A'$ triplet states are similar both for the trans and cis anions, but somewhat lower for the protonated trans ion, at 3.40, 3.39, and 2.56 eV respectively. These are all significantly lower in energy than the respective corresponding singlets. There are at present no experimental data with which these values may be compared, although comparison of the $1^3A'$ nonvertical absorption energy with the data obtained from photoacoustic calorimetry, elaborated below, is favorable.

Unremarkably, the $1^3A''$ states have virtually identical vertical excitation energies to the corresponding $1^1A''$ singlet excitations.

TABLE 10: PMCAS−CI Wavefunctions for Protonated Ionic trans-Urocanic Acid: Principal Configurations,[a] Weights and Number (weights) of Singly (S), Doubly (D), and Triply (T) Excited Configurations[b] with Coefficients Larger than 0.05

	principal configurations	%	no. of configurations (weights)		
state			S	D	T
$1^1A'$	...4a″5a″29a′30a′6a″	85.3	3 (1.6%)	10 (4.5%)	
singlet states					
$1^1A''$	30a′ → 7a″	87.8	1 (87.8%)	2 (1.1%)	10 (5.4%)
$2^1A'$	6a″ → 7a″	74.3	5 (79.8%)	12 (8.5%)	2 (0.9%)
$3^1A'$	6a″ → 8a″	69.3	4 (75.8%)	13 (11.9%)	5 (2.0%)
$4^1A'$	5a″ → 7a″	37.2	6 (77.8%)	10 (8.4%)	3 (1.3%)
	5a″ → 8a″	29.8			
$5^1A'$	5a″ → 8a″	27.8	8 (65.8%)	19 (19.4%)	5 (2.8%)
	5a″ → 7a″	20.9			
$6^1A'$	5a″6a″ → 7a″	37.0	3 (13.5%)	17 (68.5%)	8 (4.3%)
	5a″6a″ → 7a″8a″	10.4			
triplet states					
$1^3A'$	6a″ → 7a″	36.8	9 (80.1%)	13 (6.6%)	2 (0.7%)
	6a″ → 8a″	12.9			
	4a″ → 7a″	12.8			
$2^3A'$	5a″ → 7a″	65.5	10 (87.4%)	2 (0.6%)	4 (1.3%)
	5a″ → 8a″	14.1			
$3^3A'$	3a″ → 8a″	33.0	12 (85.5%)	5 (1.7%)	3 (1.0%)
	5a″ → 10a″	14.6			
	5a″ → 7a″	12.9			
$1^3A''$	30a′ → 7a″	87.3	1 (87.3%)	1 (1.6%)	7 (4.1%)

[a] Those with weights >10%. [b] With respect to the ground-state principal configuration.

Ionic Forms of Urocanic Acid

*J. Phys. Chem. A, Vol. 104, No. 38, 2000* **8803**
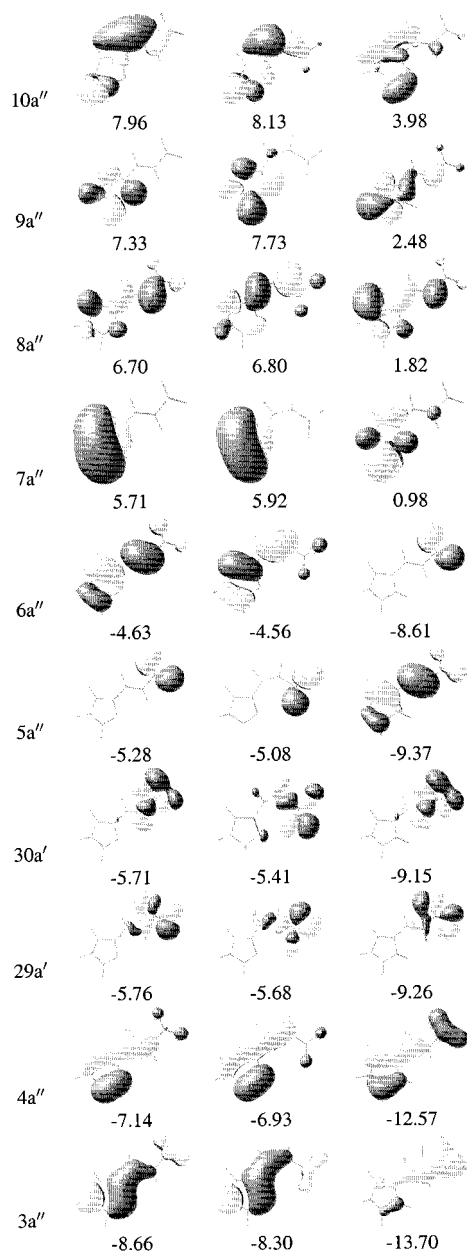
Figure 2. SCF orbital plots and energies (ANO-L basis; eV) for the six highest occupied and four lowest unoccupied MOs of anionic (left column) *trans*- and (center) *cis*-urocanic acid, and (right) protonated ionic *trans*-urocanic acid.

In summary, the computed vertical excitation energies are generally in good agreement with experiment, and certainly all lie well within the tolerances of the methods used. The broad, featureless UV absorption spectra may be thought to be due to three closely spaced $\pi\pi^*$ excited states in the trans anion, to two $\pi\pi^*$ excited states in the cis anion and to a single $\pi\pi^*$ excited state in the protonated trans species. The trans and cis anions otherwise display very similar electronic structures. In all three systems, a $\pi\pi^*$ state with a relatively low oscillator strength has been placed at ~4.0 eV, the photoexcitation energy that has been shown experimentally to lead to efficient isomerization.

3.3. Emission and Nonvertical Absorption Spectra. As noted in the Introduction, it has been found experimentally that maximum emission occurs following irradiation at 4.4−4.7 eV. The emitted wavelength is independent of pH (at least in the range pH 5.6−7.2) suggesting that radiative decay occurs from
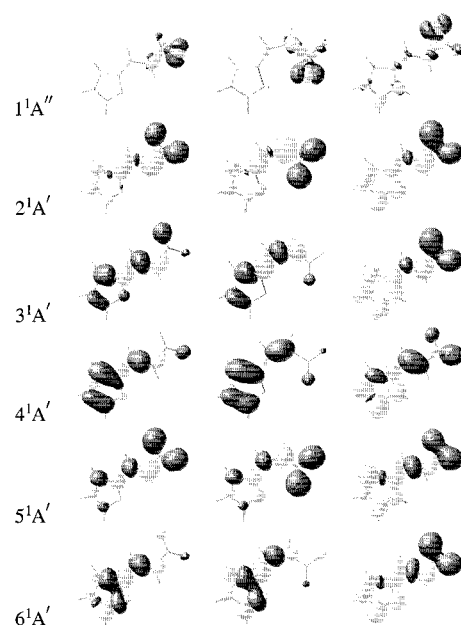

Figure 3. Electron density difference plots, relative to the ground-state density, for the respective singlet $n\pi^*$ and $\pi\pi^*$ excited states of anionic (left column) *trans*- and (center) *cis*-urocanic acid, and protonated (right) ionic *trans*-urocanic acid.
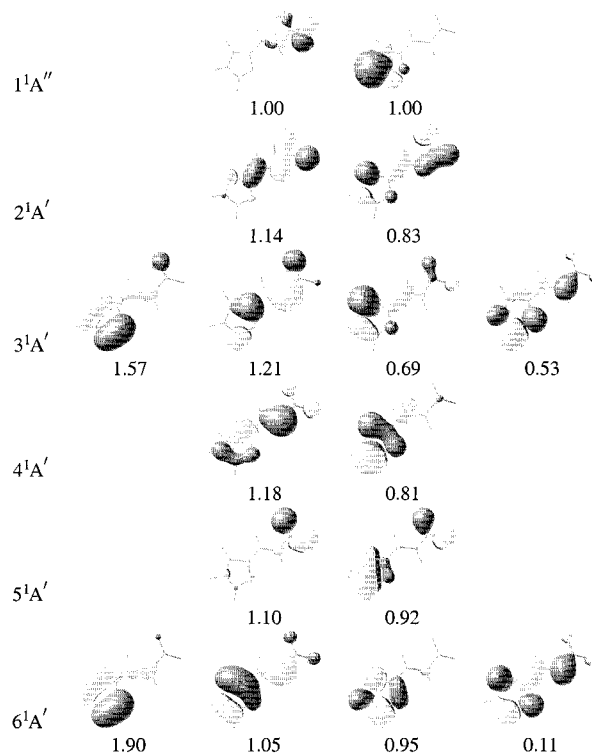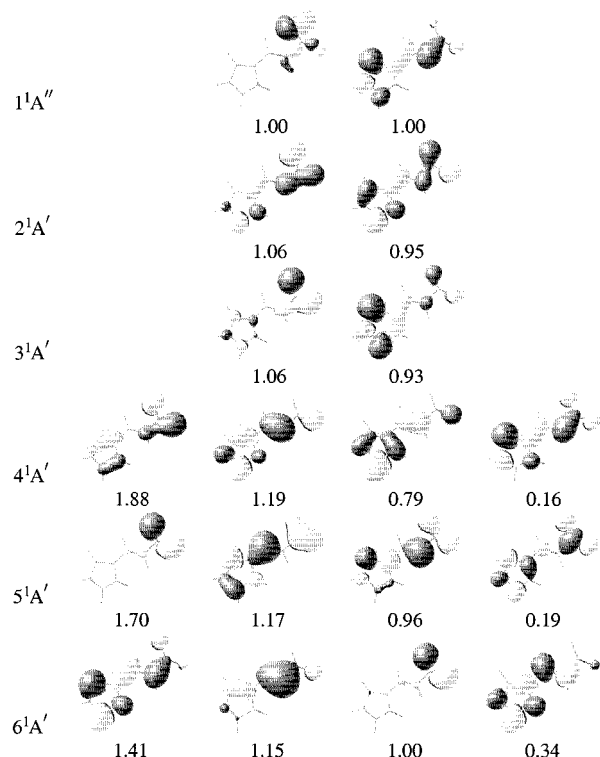

Figure 4. Plots and occupation numbers of partially occupied ($0.10 \leq$ occupancy ≤ 1.90) PMCAS−CI natural orbitals for the respective singlet $n\pi^*$ and $\pi\pi^*$ excited states of anionic *trans*-urocanic acid.

an excited state that is common to both anionic and protonated ionic species. Hanson et al. have proposed that this common excited state—the result of a $\pi\pi^*$ electronic transition—is anionic, and that the tertiary nitrogen of the protonated ion becomes deprotonated due to a reduction in the local electron density brought about by the electronic excitation.[12,14] Their experiments have further demonstrated that the lifetime of this state is short, and that it subsequently undergoes efficient

8804 *J. Phys. Chem. A, Vol. 104, No. 38, 2000*

Page et al.
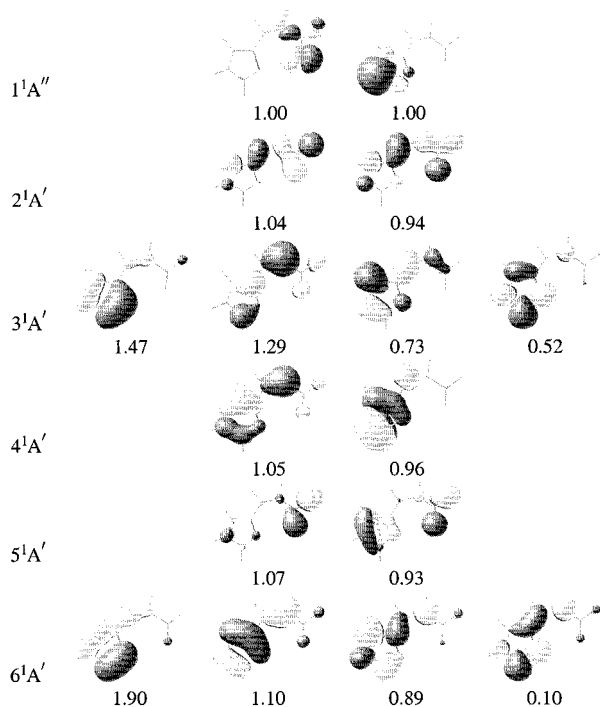
Figure 5. Plots and occupation numbers of partially occupied (0.10 ≤ occupancy ≤ 1.90) PMCAS−CI natural orbitals for the respective singlet $n\pi^*$ and $\pi\pi^*$ excited states of anionic *cis*-urocanic acid.

Figure 6. Plots and occupation numbers of partially occupied (0.10 ≤ occupancy ≤ 1.90) PMCAS−CI natural orbitals for the respective singlet $n\pi^*$ and $\pi\pi^*$ excited states of protonated ionic *trans*-urocanic acid.

intersystem crossing to the $1^3A'$ triplet. Assuming that excitation to a low-lying dark state leads to isomerization, this alternate relaxation mechanism for the spectroscopic state would in turn explain the wavelength-dependent photochemistry of urocanic acid.

TABLE 11: MS-CASPT2 Calculated Band Origins (0−0 energies, eV) and Fluorescence/Phosphorescence Maxima (eV) for *trans*- and *cis*-Urocanic Acid, and for the Protonated *trans* Species

state	0−0 energy	
trans-urocanic acid		
$1^1A''$ ($n\pi^*$)	3.13	2.07
$1^3A''$ ($n\pi^*$)	3.26	2.16
$3^1A'$ ($\pi\pi^*$)	4.03	3.66
$1^3A'$ ($\pi\pi^*$)	2.81	2.27
cis-urocanic acid		
$1^1A''$ ($n\pi^*$)	3.00	2.00
$1^3A''$ ($n\pi^*$)	3.11	1.99
$3^1A'$ ($\pi\pi^*$)	3.81	3.47
$1^3A'$ ($\pi\pi^*$)	2.80	2.27
trans-urocanic acid (protonated)		
$1^1A''$ ($n\pi^*$)	2.88	1.96
$1^3A''$ ($n\pi^*$)	2.65	1.75
$5^1A'$ ($\pi\pi^*$)	3.55	3.21
$1^3A'$ ($\pi\pi^*$)	2.44	1.52

These observations may to some extent be elucidated with a detailed comparison of the energetics of the equilibrium optimized geometries of the relevant excited states, with respect to those of the ground state.

Compiled in Table 11 are the band origins (0−0 transitions), calculated as the energy difference between the ground state and the given electronic excited state, each at their own respective equilibrium geometries, and emission maxima, calculated as the difference between the excited state and ground-state energies, both at the respective excited-state equilibrium geometry. It should be noted that the $^1A'$ geometry optimizations implicated the most intense, rather than the lowest lying, of the $\pi\pi^*$ transitions (i.e., $3^1A'$ for the two anions, and $5^1A'$ for the protonated ion).

Considering first the band origins, it can be seen that, for the trans anion, the $1^1A''$ gap is 3.13 eV (compared to 4.13 eV for the vertical excitation), the $3^1A'$ gap is 4.03 eV (cf. 4.59 eV), the $1^3A'$ gap is 2.81 eV (cf. 3.40 eV), and the $1^3A''$ gap is 3.26 eV (cf. 4.02 eV). It is immediately striking that the $3^1A'$ band origin lies ∼0.1 eV below both the $1^1A''$ and $2^1A'$ vertical excitations, raising yet further doubts that the $1^1A''$ state will be efficiently populated following irradiation at ∼4.0 eV. The 0−0 energy of the lowest lying $\pi\pi^*$ triplet is in reasonable agreement with the experimental observations of Morrison et al.,[17] and Hanson et al.,[12] which estimate its value at 2.4−2.6 eV.

Maximum emission from the $3^1A'$ state is at 3.66 eV, again in close agreement with the experimental value of 3.5 eV.[11,12] The emission maximum for the $1^1A''$ state was calculated to be 2.07 eV. As noted in the Introduction, excitation at 4.0 eV results in an emission spectrum with a maximum at 3.2 eV.[12] The unusually large discrepancy in these values may again be attributed to it being the $2^1A'$ state, rather than the $1^1A''$, that is being populated.

These computed trends are almost exactly mirrored in the cis anion, where the $1^1A''$ gap is 3.00 eV (compared to 3.81 eV for the vertical excitation), the $3^1A'$ gap is 3.81 eV (cf. 4.52 eV), the $1^3A'$ gap is 2.80 eV (cf. 3.39 eV), and the $1^3A''$ gap is 3.11 eV (cf. 3.68 eV). There are, however, no experimental data available with which to compare these.

Values calculated for the trans protonated form show a large (∼0.5 eV) red-shift in the $\pi\pi^*$ 0−0 energy relative to the trans anion, at 3.55 eV. The computed maximum fluorescence has red-shifted by a similar amount to 3.21 eV. This point is of interest with regard to the findings of Hanson et al.,[12] since it

Ionic Forms of Urocanic Acid

J. Phys. Chem. A, Vol. 104, No. 38, 2000 **8805**

must rule out the possibility that the observed pH independence of the emission spectra could be attributed to simple coincidence. The $1^3A'$ band origin is 2.44 eV, once again confirming the experimental assignment.[12]

4. Summary and Conclusions

The MS−CASPT2 excitation energies presented reveal a picture of the photochemistry of urocanic acid that is quite different to any that has previously been proposed. In both the anionic and the protonated forms, $\pi\pi^*$ singlet states with low oscillator strengths are to be found at ∼4.0 eV, with one or more strongly absorbing $\pi\pi^*$ singlets occurring in the range 4.5−5.0 eV. These data are fully consistent with experimental measurements, which show maximum absorption in the range 4.4−4.7 eV.

The excitation energy of the lowest lying $n\pi^*$ singlet state varies considerably between the trans anion and its protonated analog, being almost 1.0 eV lower in the latter.

As noted in the Introduction, it has been found experimentally that trans → cis isomerization takes place following photo-excitation at ∼4.0 eV. Although the computed $1^1A''$ vertical transition has indeed been placed at ∼4.0 eV for the two anions—supporting the mechanism suggested by Li et al., implicating the $n\pi^*$ singlet—it seems more likely, on the basis of the present evidence, that the initial step is a $\pi\pi^*$ transition. What is not clear at this time, however, is whether isomerization takes place in the singlet manifold, or whether it follows consequentially from intersystem crossing to the triplet manifold, along a path similar to that found by Merchán and González-Luque for retinal.[38] Computation of potential energy curves for each of the possible minimum energy paths for the photoisom-erisation is currently in progress.

References and Notes

(1) Morrison, H.; Deibel, R. M. *Photochem. Photobiol.* **1986**, *43*, 663−665 and references therein.

(2) Mohammad, T.; Morrison, H.; HogenEsch, H. *Photochem. Photobiol.* **1999**, *69*, 115−135 and references therein.

(3) Black, H. S.; de Gruijl, F. R.; Forbes, P. D.; Cleaver, J. E.; Ananthaswamy, H. N.; deFabo, E. C.; Ullrich, S. E.; Tyrrell, R. M. *J. Photochem. Photobiol., B* **1997**, *40*, 29−47 and references therein.

(4) Morrison, H. *Photoderm.* **1985**, *2*, 158−165.

(5) deFabo, E. C.; Noonan, F. P. *J. Exp. Med.* **1983**, *158*, 84−98.

(6) Reeve, V. E.; Greenoak, G. E.; Canfield, P. J.; Boehm-Wilcox, C.; Gallagher, C. H. *Photochem. Photobiol.* **1989**, *49*, 459−464.

(7) Noonan, F. P.; deFabo, E. C.; Kripke, M. L. *Photochem. Photobiol.* **1981**, *34*, 683−689.

(8) Norval, M.; Gibbs, N. K.; Gilmour, J. *Photochem. Photobiol.* **1995**, *62*, 209−217.

(9) Mehler, A. H.; Tabor, H. *J. Biol. Chem.* **1955**, *201*, 755−784.

(10) Öhman, H.; Vahlquist, A. *Acta Dermato−Venereolog.* **1994**, *74*, 375−379.

(11) Shukla, M. K.; Mishra, P. C. *Spectrochim. Acta* **1995**, *51*, 831−838.

(12) Hanson, K. M.; Li, B. L.; Simon, J. D. *J. Am. Chem. Soc.* **1997**, *119*, 2715−2721.

(13) Morrison, H.; Bernasconi, C.; Pandey, G. *Photochem. Photobiol.* **1984**, *40*, 549−550.

(14) Li, B. L.; Hanson, K. M.; Simon, J. D. *J. Phys. Chem.* **1997**, *101*, 969−972.

(15) Hanson, K. M.; Simon, J. D. *Photochem. Photobiol.* **1998**, *67*, 538−540.

(16) Ullman, E. F.; Babad, E.; Sung, M. *J. Am. Chem. Soc.* **1969**, *91*, 5792−5796.

(17) Morrison, H.; Avnir, D.; Bernasconi, C.; Fagan, G. *Photochem. Photobiol.* **1980**, *32*, 711−714.

(18) Laihia, J. K.; Lemmetyinen, H.; Pasanen, P.; Jansen, C. T. *J. Photochem. Photobiol.*, **1996**, *33*, 211−217.

(19) Lewis, F. D.; Yoon, B. A. *Res. Chem. Intermed.* **1995**, *21*, 749−763.

(20) Lahti, A.; Hotokka, M.; Neuvonen, K.; Karlström, G. *J. Mol. Struct. (THEOCHEM)* **1998**, *452*, 185−202.

(21) Page, C. S.; Merchán, M.; Serrano-Andrés, L.; Olivucci, M. *J. Phys. Chem. A* **1999**, *103*, 9864−9871.

(22) Lahti, A.; Hotokka, M.; Neuvonen, K.; Ayras, P. *Struct. Chem.* **1997**, *8*, 331−342.

(23) Lahti, A.; Hotokka, M.; Neuvonen, K.; Karlström, G. *Int. J. Quantum Chem.* **1999**, *72*, 25−37.

(24) Andersson, K.; Malmqvist, P.-Å.; Roos, B. O.; Sadlej, A. J.; Wolinski, K. *J. Phys. Chem.* **1990**, *94*, 5483−5488.

(25) Andersson, K.; Malmqvist, P.-Å.; Roos, B. O. *J. Chem. Phys.* **1992**, *96*, 1218−1226.

(26) Widmark, P.-O.; Malmqvist, P.-Å.; Roos, B. O. *Theor. Chim. Acta* **1990**, *77*, 291−306.

(27) Merchán, M.; Serrano-Andrés, L.; Fülscher, M. P.; Roos, B. O. Multiconfigurational Perturbation Theory Applied to Excited States of Organic Compounds. In *Recent Advances in Multireference Methods*; Hirao, K., Ed.; World Scientific Publishing Company: Amsterdam, 1998.

(28) The ANO-L basis sets are, by design, optimised for the study of the valence states of neutral, anionic and cationic species. Addition of atom-centred diffuse functions was examined, but required unreasonably high integral accuracy to avoid linear dependencies in the CASSCF. The results were nevertheless essentially invariant. When a set of molecule-centred 1s1p1d diffuse functions was added, diffuse states described by a singly excited configuration were obtained In addition to the valence anion states. These solutions simulate the neutral molecule and a free electron by placing the extra electron into the most diffuse orbital. The computed energy for this state is strongly dependent on the diffuseness of the basis set employed. Such unstable solutions should be discarded.[39,40]

(29) Finley, J.; Malmqvist, P. Å.; Roos, B. O.; Serrano-Andrés, L. *Chem. Phys. Lett.* **1998**, *288*, 299−306.

(30) Roos, B. O. The Complete Active Space Self-Consistent Field Method and its Applications in Electronic Structure Calculations. In *Advances in Chemical Physics*: *Ab Initio Methods in Quantum Chemistry II*; Lawley, K. P., Ed.; John Wiley & Sons Ltd.: Chichester, England, 1987.

(31) Malmqvist, P.-Å. *Int. J. Quantum Chem.* **1986**, *30*, 479−494.

(32) Malmqvist, P. Å.; Roos, B. O. *Chem. Phys. Lett.* **1989**, *155*, 189−194.

(33) Roos, B. O.; Fülscher, M. P.; Malmqvist, P.-Å.; Merchán, M.; Serrano-Andrés, L. Theoretical Studies of Electronic Spectra of Organic Molecules. In *Quantum Mechanical Electronic Structure Calculations with Chemical Accuracy*; Langhoff, S. R., Ed.; Kluwer Academic Publishers: Dordrecht, The Netherlands, 1995.

(34) Roos, B. O.; Andersson, K.; Fülscher, M. P.; Malmqvist, P.-Å.; Serrano-Andrés, L.; Pierloot, K.; Merchán, M. Multiconfigurational Perturbation Theory: Applications in Electronic Spectroscopy. In *Advances in Chemical Physics*: *New Methods in Computational Quantum Mechanics*; Prigogine, I., Rice, S. A., Eds.; John Wiley & Sons: New York, 1996; Vol. XCIII.

(35) Andersson, K.; Blomberg, M. R. A.; Fülscher, M. P.; Karlström, G.; Lindh, R.; Malmqvist, P.-Å.; Neogrády, P.; Olsen, J.; Roos, B. O.; Sadlej, A. J.; Schütz, M.; Seijo, L.; Serrano-Andrés, L.; Siegbahn, P. E. M.; Widmark, P.-O. *MOLCAS*, Version 4; Department of Theoretical Chemistry: University of Lund, P.O. Box S-221 00 Lund, Sweden, 1997.

(36) Frisch, M. J.; Trucks, G. W.; Schlegel, H. B.; Gill, P. M. W.; Johnson, B. G.; Robb, M. A.; Cheeseman, J. R.; Keith, T.; Petersson, G. A.; Montgomery, J. A.; Raghavachari, K.; Al-Laham, M. A.; Zakrzewski, V. G.; Ortiz, J. V.; Foresman, J. B.; Cioslowski, J.; Stefanov, B. B.; Nanayakkara, A.; Challacombe, M.; Peng, C. Y.; Ayala, P. Y.; Chen, W.; Wong, M. W.; Andres, J. L.; Replogle, E. S.; Gomperts, R.; Martin, R. L.; Fox, D. J.; Binkley, J. S.; Defrees, D. J.; Baker, J.; Stewart, J. J. P.; Head-Gordon, M.; Gonzalez, C.; Pople, J. A. *Gaussian 94*, Revision B.1; Gaussian, Inc.: Pittsburgh, PA, 1995.

(37) Bifone, A.; de Groot, H. J. M.; Buda, F. *Chem. Phys. Lett.* **1996**, *248*, 165−172.

(38) Merchán, M.; González-Luque, R. *J. Chem. Phys.* **1997**, *106*, 1111−1122.

(39) Rubio, M.; Merchán, M.; Ortí, E. *J. Phys. Chem.* **1995**, *99*, 14980−14987.

(40) Pou-Amérigo, R.; Serrano-Andrés, L.; Merchán, M.; Ortí, E. *J. Am. Chem. Soc.* **2000**. In press.